Pharm Res (2015) 32:2372–2383
DOI 10.1007/s11095-015-1630-5

RESEARCH PAPER

Synthesis and Evaluation of Mesoporous Carbon/Lipid Bilayer Nanocomposites for Improved Oral Delivery of the Poorly Water-Soluble Drug, Nimodipine

Yanzhuo Zhang • Qinfu Zhao • Wufu Zhu • Lihua Zhang • Jin Han • Qisi Lin • Fengwei Ai

Received: 27 October 2014 / Accepted: 14 January 2015 / Published online: 22 January 2015

ABSTRACT

Purpose A novel mesoporous carbon/lipid bilayer nanocomposite (MCLN) with a core-shell structure was synthesized and characterized as an oral drug delivery system for poorly water-soluble drugs. The objective of this study was to investigate the potential of MCLN-based formulation to modulate the *in vitro* release and *in vivo* absorption of a model drug, nimodipine (NIM).

Methods NIM-loaded MCLN was prepared by a procedure involving a combination of thin-film hydration and lyophilization. Scanning electron microscopy (SEM), transmission electron microscopy (TEM), specific surface area analysis, differential scanning calorimetry (DSC) and X-ray diffraction (XRD) were employed to characterize the NIM-loaded MCLN formulation. The effect of MCLN on cell viability was assessed using the MTT assay. In addition, the oral bioavailability of NIM-loaded MCLN in beagle dogs was compared with that of the immediate-release formulation, Nimotop®.

Results Our results demonstrate that the NIM-loaded MCLN formulation exhibited a typical sustained release pattern. The NIM-loaded MCLN formulation achieved a greater degree of absorption and longer lasting plasma drug levels compared with the commercial formulation. The relative bioavailability of NIM for NIM-loaded MCLN was 214%. MCLN exhibited negligible toxicity.

Conclusion The data reported herein suggest that the MCLN matrix is a promising carrier for controlling the drug release rate and improving the oral absorption of poorly water-soluble drugs.

KEY WORDS drug absorption · lipid bilayer · mesoporous carbon · nano-drug delivery system · sustained release

ABBREVIATIONS

APIs	Active pharmaceutical ingredients
DSC	Differential scanning calorimetry
LPNs	Lipid enveloped polymeric nanoparticles
MC	Mesoporous carbon
MCLN	Mesoporous carbon/lipid bilayer nanocomposite
NIM	Nimodipine
SEM	Scanning electron microscopy
TEM	Transmission electron microscopy
XRD	X-ray diffraction

INTRODUCTION

Generally, the oral route is the most readily accepted route for drug delivery. Because of the smaller bulk, greater stability, precise dosage and easy application, solid oral dosages forms have many advantages over other types of oral dosage forms. Therefore, most of active pharmaceutical ingredients (APIs) under development these days are intended to be used as solid

Electronic supplementary material The online version of this article (doi:10.1007/s11095-015-1630-5) contains supplementary material, which is available to authorized users.

Y. Zhang (✉) • L. Zhang • J. Han • Q. Lin • F. Ai
Jiangsu Key Laboratory of New Drug Research and Clinical Pharmacy
Xuzhou Medical College P.O. Box 62, No. 209, Tongshan Road
Xuzhou 221004, China
e-mail: yanzhuozhang@126.com

Q. Zhao
School of Pharmacy Shenyang Pharmaceutical University
Shenyang 110016, China

W. Zhu
School of Pharmacy Jiangxi Science and Technology Normal University
Nanchang 330013, China

dosage forms. However, over 40% of newly developed APIs that are being developed today by high-throughput screening and combinatorial chemistry fall into biopharmaceutical classification system (BCS) classes II (low-solubility, high-permeability) and IV (low-solubility, low-permeability) [1, 2]. APIs with poor aqueous solubility often demonstrate poor and erratic absorption when administrated orally due to their dissolution rate-limiting absorption in the gastrointestinal tract. Hence, one of the major challenges for the pharmaceutical industry is to develop strategies to improve the aqueous solubility and dissolution rate of poorly water-soluble drugs [3, 4]. In other cases, for many hydrophobic APIs with a short elimination half-life and a low therapeutic index, it is necessary to administer them regularly, at frequent intervals in order to maintain the concentration within the therapeutic range. Therefore, considerable research has been conducted into methods of improving the solubility and modulating the dissolution rate to increase the oral bioavailability of poorly water-soluble drugs [5, 6]. Over recent decades, various nanonization strategies have been proposed to increase the aqueous solubility and regulate the dissolution rate of poorly water-soluble drugs. These strategies include reducing the particle size to increase the surface area [3, 7], using cyclodextrin inclusion complexes or solid lipid nanoparticles [8, 9], solubilization in surfactant systems and developing novel nano-drug delivery systems for sustained release [10–13].

During the past few years, lipid enveloped polymeric nanoparticles (LPNs) have emerged as a robust and promising drug and gene delivery system. LPNs synergistically combine favorable features of both polymeric nanoparticles with physical stability and liposomes with biomimetic characteristics [14–16]. Various therapeutic agents, such as drugs, genes and proteins, can be encapsulated inside the solid polymeric core while the lipid layer (with or without therapeutic agents) confers biocompatibility and biomimetic properties to the polymeric core. In addition, LPNs-based drug delivery systems may improve the biological response to many drug molecules, especially by modulating their pharmacokinetics and thereby offering many advantages such as prolonged drug absorption and significantly reduced side effects [16–19]. For a sustained release, different kinds of polymers or lipids, such as phospholipids, polydiacetylene and poly (ε-caprolactone) derivatives, may be used to modulate the release rate of the encapsulated drugs [15, 18, 20]. However, polymeric nanoparticles are usually ill suited for encapsulation of large amounts of relatively hydrophilic drugs [21, 22]. Notably, mesoporous carbon (MC) materials as prospective drug carriers for oral drug delivery have recently attracted much attention. Compared with polymeric nanoparticles, ordered MC nanomatrices offer several advantages for drug delivery, including unique ordered porosity at the nanoscale, a large inner surface area and pore volume to highly disperse the drug molecules, provide a high drug loading capacity, with tunable pore structures and pore sizes to control release of the incorporated drug molecules and excellent physicochemical stability [23–25]. Therefore, it would be very useful to construct a new type of lipid enveloped MC nanoparticles, MCLN, with a core-shell structure as an oral nano-drug delivery system for poorly water-soluble drugs. Compared with traditional liposomes, MCLN may be more stable with the advantage of the nanoporous core to control both drug loading and release. Compared with pure MC nanoparticles, MCLN may be more biocompatible and have the additional benefit of the lipid bilayers to reduce or eliminate the initial burst release of encapsulated drugs and reduce drug leakage [17, 18]. However, until now, no study has explored their potential in modulating the dissolution rate and improving the bioavailability of poorly water-soluble drugs following oral administration.

In this study, we have designed a new type MCLN as an oral drug delivery system where monodisperse MC was used as the core containing a poorly water-soluble drug enveloped by lipid bilayers as the hydrophobic shell. To increase the storage stability of the lipid bilayers, the drug-loaded MCLN were freeze-dried. NIM is one of the dihydropyridine calcium channel blockers recommended for the prevention and treatment of delayed ischaemic neurological disorders which often occur in patients with subarachnoid hemorrhages [26]. However, NIM is classified as a BCS Class II drug. The absolute bioavailability after oral administration of the solid dosage form of NIM is approximately 5–15% mainly due to its low aqueous solubility and extensive first-pass metabolism [27–29]. In addition, NIM requires frequent dosing (every 4 h) because of its rapid elimination. The inconvenience of frequent dosing can often results in poor patient compliance. Therefore, improving the solubility and modulating the dissolution rate of such a drug is expected to enhance its bioavailability, provide a more uniform therapeutic effect over time, and improve patient compliance. Our primary aim was to regulate the *in vitro* dissolution and improve the *in vivo* absorption of NIM by means of MCLN-based nanoparticles. To achieve this goal, the NIM-loaded MCLN formulation was characterized in terms of its morphology, inner structure, mean particle size, pore volume, specific surface area, drug loading, physical state, solubility, *in vitro* release behavior and amorphous state stability. Furthermore, a comparative bioavailability study was performed on the NIM-loaded MCLN formulation in fasted beagle dogs and compared with a conventional immediate release tablet of NIM. In addition, the cytotoxic effects of MCLN on Caco-2 and HT-29 cells were also evaluated using MTT assay.

MATERIALS AND METHODS

Materials

Pluronic F127 was provided by BASF (Ludwigshafen, Germany). Phenol and formalin were purchased from Aladdin (Shanghai, China). Coarse NIM (purity ≥98%) was

kindly donated from Xinhua Pharma (Shandong, China). 1,2-dipalmitoyl-sn-glycero-3-phosphocholine (DPPC) and 1,2-dioleoyl-3-trimethylammonium propane (DOTAP) were purchased from Avanti Polar Lipids Inc. (Alabaster, AL, USA). Fetal bovine serum (FBS), Dulbecco's modified Eagle's medium (DMEM) and 3-(4,5-Dimethylthiazol-2-yl)-2,5-diphenyltetrazolium bromide (MTT) were obtained from Sigma-Aldrich (St. Louis, MO, USA). Distilled water purified using a DW 200 purification system (Hitech Instruments, Shanghai, China) was used throughout this study. Commercially available NIM preparation (Nimotop®, Bayer Pharma, Germany) was chosen as the reference in the bioavailability study. Simulated gastric fluid (SGF, pH1.2) and simulated intestinal fluid (SIF, pH6.8) were prepared according to the USP procedure. All the other reagents and chemicals used were of analytical grade or better.

Cell line

The human colorectal carcinoma cell lines, Caco-2 and HT-29 (American Type Culture Collection, Manassas, VA, USA), were grown in DMEM supplemented with 1% nonessential amino acids, 10% fetal bovine serum, 1% L-glutamine, 100 U/ml penicillin and 100 μg/ml streptomycin. Cultures were maintained in a humidified atmosphere at 37°C with 5% CO_2 (BBD 6220 CO_2 Incubator, Thermo Scientific, Germany). The growth medium was changed every 2–3 days until the time of use.

Preparation of MC Nanospheres

The ordered MC nanospheres were synthesized using Pluronic F127 as a soft-template and phernolic resol as a carbon precursor, as reported by Li and co-workers with some modifications [30]. In brief, 0.4 g phenol, 1.2 ml formalin aqueous solution (37 wt.%) and 10 ml sodium hydroxide solution (0.1 M) were mixed and stirred at 70°C for 2 h. Then, 30 ml distilled water was added to the mixture and stirred for 10 h to obtain a phernolic resol solution. After cooling to room temperature, the obtained phernolic resol solution was mixed with 10.5 ml Pluronic F127 aqueous solution (6 wt.%) and stirred magnetically for 2 h at 70°C to obtain phernolic resol-Pluronic F127 composite micelles. The stirring speed was set at 300 rpm. Next, the above mixture was transferred to a Teflon-coated autoclave and diluted with 120 ml distilled water. After that, the autoclave was placed in an oven for hydrothermal treatment at 150°C for 10 h. The resulting solid was then collected by centrifugation (9000×g, 20 min), washed with ethanol and dried at 25°C in a LG0612K quartz tubular oven (Zhongke, China). Finally, the as-prepared product was carbonized at 900°C for 4 h (heating rate 2°C/min) under a pure nitrogen atmosphere to obtain the ordered MC nanospheres.

Preparation of NIM-Loaded MC

The model drug NIM was loaded into the nanopores of MC using the solvent immersion/evaporation procedure [23]. In brief, weighed quantities of MC nanoparticles powder (3.5 g) and NIM (2.5 g) were added to 20 ml acetone. After ultrasonication for 5 min, the resultant mixture was agitated in a dark place at 20°C for 6 h using a rotary mixer (50 rpm) to achieve maximum loading of MC in the pore channels. Next, the obtained NIM-impregnated MC particles were separated from the drug solution by vacuum filtration through a polypropylene membrane filter (Pall, USA) with a 0.1 μm pore size. Finally, the filtered wet particles were dried at 50°C under reduced pressure (0.75 Torr) for more than 1 day in order to remove the solvent completely. The obtained NIM-loaded MC powder was labeled as NIM-MC.

Self-Assembly of Lipid-Enveloped NIM-MC

Lipid-enveloped NIM-MC core-shell nanoparticles were prepared by a procedure involving a combination of thin-film hydration and lyophilization. In a typical synthesis procedure, a lipid mixture, composed of 13 mg DOTAP, 6 mg DPPC and 1.2 mg cholesterol, was dissolved in 20 ml chloroform in a round bottom flask and dried in a N-1001rotary evaporator (Eyela, Japan) under reduced pressure at 40°C to form a thin lipid film. Meanwhile, an accurately weighed amount of NIM-MC (about 100 mg) was dispersed in 10 mM phosphate buffered saline (PBS, pH 7.4, 20 ml) and vortexed for 2 min to form a NIM-MC dispersion. Next, 20 ml NIM-MC dispersion was added to hydrate the resulting thin lipid film at 25°C to obtain a lipid-enveloped NIM-MC suspension. After ultrasonication for 2 min, the obtained suspension was extruded three times through Nuclepore® polycarbonate membranes with an initial pore diameter of 0.45 and then 0.22 μm pore diameters (Whatman, UK) using a mini-extruder. Then, the lipid-enveloped NIM-MC nanocomposites were separated from the blank liposomal suspension by centrifugation at 21000×g for 2 min. The centrifuged particles were washed with PBS, transferred to borosilicate lyophilization vials, and lyophilized in an Alpha 1-2LD Plus freeze-dryer (Christ, Germany). The lyophilization program was conducted as follows: Typically, the primary freezing temperature was −40°C for 3 h. Then, primary drying was carried out at a shelf temperature of −20°C and a chamber pressure of 60 mTorr for 8 h. Finally, the shelf temperature was raised to 25°C for 3 h. The heating and cooling rate was 1°C /min. The lyophilized composite samples were labeled as NIM-MCLN.

Physico-Chemical Characterization of Drug-Loaded Nanoparticles

SEM Study

To study the surface morphology, the unloaded MC, NIM-MC and freeze-dried NIM-MCLN particles were coated with a layer of Au-Pd using a K550X sputter coater (Emitech Ltd., UK), and observed under a JSM-6301 F field emission scanning electron microscope (JEOL, Japan) operated at 15 kV.

TEM Study

TEM images of the prepared samples were captured using a JEM-2100 field emission gun microscope (JEOL, Japan) equipped with an Oxford spectrometer and Gatan digital imaging system operated at 200 kV. Samples for TEM imaging were prepared by placing a drop of the particle suspension in water on a 200-mesh copper TEM grid and drying at room temperature.

Particle Size and Zeta Potential Analysis

The particle size and zeta-potential of the prepared nanoparticles was determined using a Nicomp^{TM}380 Zeta potential/particle sizer (Particle Sizing System, USA), after dispersing the nanoparticles in distilled water. Measurements were carried out at 25°C.

Specific Surface Area and Pore Volume Analysis

Nitrogen sorption isotherms and pore characterization of the prepared samples were recorded at −196°C using an ASAP Tristar 3000 surface area and pore size analyzer (Micromeritics, USA). Prior to analysis, each powder sample (around 0.1 g) was evacuated at a pressure of 0.3 mTorr at 40°C overnight to remove physically adsorbed water. The specific surface area (S_{BET}) was calculated using the Brunauer-Emmett-Teller (BET) equation. The average pore diameter was obtained from the adsorption branch of the isotherm using the Barrett-Joyner-Halenda (BJH) method [25].

XRD Study

The degree of crystallinity of the loaded NIM was estimated by XRD. XRD patterns of the prepared samples were collected using an AXS D8 Advance diffractometer (Bruker AXS GmbH, Germany) equipped with Cu Kα radiation (λ= 1.542 Å). A copper anode tube was used at 40 mA and 30 kV. The data were recorded from 5 to 40° (2θ) with a step size of 0.010° (2θ).

DSC Study

Thermal response profiles of each sample were recorded on a differential scanning calorimeter (Q2000, TA Instruments, USA). The instrument was calibrated with indium as a reference. Samples were prepared by weighing about 7 mg into an aluminum pan, which was then covered with a pierced aluminum lid. The sample cells were heated from 30 to 250°C at 10°C/min and purged with dry nitrogen at a flow rate of 50 ml/min.

HPLC Analysis of NIM *in Vitro*

HPLC was employed for drug analysis. The chromatographic system used was an Agilent Chromatograph (Agilent Technologies, USA) equipped with a quaternary pump, model G1311A, a variable wavelength detector, model G1314B, a column oven, model G1316A, and an autosampler, model G1329A. A 250×4.6 mm reversed-phase Zorbax C_{18} analytical column was used for chromatographic separation. The mobile phase, methanol: acetonitrile: water (35:38:27, v/v/v), was pumped isocratically at 1.0 ml/min. A sample aliquot of 10 µl was injected and the effluent monitored at 237 nm. The peak area response to the concentration of NIM was linear over the range of 0.1–20 µg/ml (r^2=0.99).

Drug Loading Capacity

The drug loading capacity, expressed as the mass of encapsulated NIM divided by the mass of composites, as a percentage, was determined by solvent extraction. Briefly, an accurately weighed amount of NIM-loaded composite (about 10 mg) was dispersed in 200 ml methanol. The resulting suspension was ultrasonicated for 15 min, transferred to a rotary mixer for 12 h, then, the porous matrix was separated from the NIM solution by centrifugation (6000×g, 10 min). The supernatant was passed through a 0.1 µm cellulose acetate filter, suitably diluted with mobile phase and then the drug concentration was determined by HPLC. All measurements were performed in triplicate.

Aqueous Solubility Study

Solubility experiments were performed with pure NIM and all test formulations using the Higuchi and Connor method [31]. Briefly, an excess amount of NIM formulation was dispersed in 20 ml solvent (purified water or PBS) and vortexed for 2 min to form a coarse suspension which was transferred to a screw-capped glass tube and incubated in a shaking air bath operated at 50 rpm and 37°C. After 48 h incubation, a 2 ml aliquot of the incubated sample was passed through a 0.1 µm cellulose acetate filter, and diluted with a suitable volume of

methanol prior to measuring the drug concentration by HPLC.

In Vitro Drug Release Testing

Drug release testing of each NIM formulation was conducted with an AT7 Smart automated dissolution apparatus (Sotax, Switzerland). The USP Dissolution Apparatus 2 paddle method was used at a rotational speed of 100 rpm. Each prepared sample or crude drug powder, equivalent to 30 mg NIM, was added to the dissolution vessels containing 900 ml release medium at 37±0.5°C. SGF (pH1.2), SIF (pH6.8) and purified water containing 0.3 wt.% sodium dodecyl sulfate (SDS) were used as different release media. During testing, 5 ml aliquots of release medium were removed from the dissolution vessels and replaced with an equal volume of fresh release medium after 0.5, 1, 2, 4, 6, 8, 10, 12 and 24 h. Samples were immediately passed through a 0.1 μm cellulose acetate filter and diluted with mobile phase. The amount of NIM dissolved in the release media was determined by HPLC. All the tests were carried out in triplicates.

In Vitro Cytotoxicity Assay

The cytotoxicity of the prepared nanoparticles (MCLN and MC) towards Caco-2 and HT-29 cells was evaluated by an MTT conversion assay. Briefly, Caco-2 (or HT-29) cells were seeded into 96-well microtiter plates at a density of 1×10^4 cells per well and incubated for about 72 h to reach confluence. Then, the culture medium in the wells was removed and replaced with fresh DMEM (100 μl) containing different concentrations (10–200 μg/ml) of MCLN (or MC). Control cells were cultured with blank culture medium alone. At the end of the incubation period (12 or 48 h), the culture medium, with or without the test nanoparticles in each well, was removed and replaced with fresh DMEM (100 μl) containing 10% MTT. After the cells were incubated for another 4 h, the MTT medium was removed, and 100 μl dimethyl sulfoxide was added to each well to dissolve precipitated formazan crystals. Finally, the absorbance of the resulting formazan solution was measured using a microplate reader (Synergy^{TM} HT, BioTek Instruments Inc, USA) at 570 nm, and the cell viability was calculated as: Absorbance of samples×100/Absorbance of control.

In Vivo Absorption Studies

Animals and Drug Administration

A pharmacokinetic study in beagle dogs was designed to evaluate the NIM-loaded MCLN formulation by comparison with the commercially available solid dispersion formulation, Nimotop®. All the procedures used in the present study were carried out in accordance with the Guidelines for Animal Experimentation of Xuzhou Medical College. Six beagle dogs (10–12 kg) were divided into two groups, and a single-dose, randomized, crossover study was carried out with a washout period of 7 days. After an overnight fast, each formulation containing 60 mg NIM was given to the dogs (as a single dose equivalent to 5–6 mg/kg) with 100 ml water. At designated times (pre-dosing and 0.5, 1, 1.5, 2, 3, 4, 6, 8, 10, 12 and 24 h post-dosing), serial blood samples (about 2 ml each) were collected from each animal by venepuncture and then transferred to heparinized Eppendorf tubes. After collection (within 1 h), the plasma was separated from samples by centrifugation (2000×g, 15 min) at 4°C and stored at −20°C until further analysis.

Determination of NIM in Plasma

The NIM content in plasma was assayed using a Waters 2695 HPLC system (Waters, USA) consisting of a binary pump, model 1525, and a dual wavelength absorbance detector (237 nm), model 2487. Chromatographic separation of NIM was performed on a 150×4.6 mm Shim-pack VP-ODS C_{18} column with a security guard column (Shimadzu, Japan) at 35°C, eluting with a mixture of methanol/water/triethylamine (65:35:0.02) as the mobile phase at a flow rate of 1.0 ml/min. Prior to HPLC analysis, an aliquot of 200 μl of each plasma sample was transferred to a centrifuge tube along with 20 μl internal standard (nitrendipine, 2.5 μg/ml) in the mobile phase and 100 μl sodium hydroxide solution (0.5 M). After vortex-mixing for 0.5 min, the mixture was extracted with 3 ml anhydrous ether and *n*-hexane (50:50) by vortex-mixing for 4 min. After centrifugation at 6000×g for 10 min, the upper organic phase was transferred to a clean centrifuge tube and evaporated using a rotatory centrifugal vacuum concentrator. The residue was then reconstituted with 0.1 ml methyl alcohol and a 20 μl aliquot of the resulting solution was injected into the HPLC system for analysis. The calibration curve was linear with a correlation coefficient of 0.99 over the range of 5–1000 ng/ml. The limit of detection and the limit of quantitation was 2 and 5 ng/ml, respectively. The accuracy (percentage difference from nominal) of the quality control samples (5, 50 and 1000 ng/ml) used during sample analysis ranged from 3.8 to 10.6%, with a precision (as measured by the percentage relative standard deviation) of <11.0%. The method had an acceptable recovery of 76.3±4.2% for NIM.

Pharmacokinetic Analysis

The pharmacokinetic parameters based on non-compartmental approach were calculated using Drug and Statistics software (version 2.1, Mathematical Pharmacology Professional Committee of China). The area under the plasma

concentration–time curve from time zero to time t h, ($AUC_{0\rightarrow t}$), was obtained by the linear and log-linear trapezoidal method. The peak plasma concentration of drug (C_{max}) and the time taken to reach C_{max} (T_{max}) were obtained directly from the plasma *vs.* time profile. The relative bioavailability was calculated as the ratio of AUC_{0-24h} values between the NIM-MCLN formulation and the commercial formulation.

Physical Stability Test

A stability study was carried out on the NIM formulation in accordance with ICH accelerated stress-stability conditions. Each sample was put into a glass vial protected from light and sealed, which was then stored (40°C, 75% RH) in a chamber kept at a constant temperature and humidity. The samples were obtained after designated incubation times (1, 3 and 6 months), and the crystallinity and particle size of the samples were monitored. The *in vitro* drug release curves and solubility were also compared before and after storage.

Statistical Analysis

All results were expressed as an average ± standard deviation (SD) from at least three independent experiments. For statistical analysis, a Student's *t*-test or one-way analysis of variance (ANOVA) test was used. Statistical significance was defined as $p < 0.05$.

RESULTS AND DISCUSSION

Morphology and Structure Characterization

The SEM and TEM micrographs provide important details of the surface morphology, particle size and inner structure. As shown in Fig. 1A, the prepared pure MC particles consist of many monodisperse, roughly spherical nanoparticles with an average diameter of about 170 nm and a smooth surface. The corresponding TEM image, as shown in Fig. 1B, clearly shows their highly ordered mesoporous structure. The pore size of MC estimated from the TEM image was approximately 3–4 nm, which was in agreement with the results from the nitrogen adsorption measurements (Table I). According to the SEM observation, the raw NIM was found to be cubic in shape and the particle size was around 5–50 μm (Fig. S1, Supporting Information). A representative SEM image (Fig.1C) revealed that the drug-loaded MC possesses a similar morphology to pure MC, and no separate particles of drug crystals were present. However, the TEM micrograph of the drug-loaded MC shown in Fig. 1D shows that the mesoporous structures are not as clear as in the case of unloaded MC (with a clear contrast between the matrix and the mesoporous channels), indicating that most of the mesopores were filled with the model drug. Interestingly, the freeze-dried drug-loaded MCLN particles still retain the morphological features of pure MC except for having a much rougher surface due to the surface change caused by the thin lipid coating (Fig.2A). As can be clearly seen from Fig. 2B, the drug-loaded MCLN particles show obvious core-shell structures, light lipid shells coat the dark drug-loaded MC cores, and these core-shell nanocomposites are relatively monodisperse. Dynamic light scattering (DLS) measurements showed that the mean particle size of NIM-loaded MCLN was 196 ± 35 nm, which is in agreement with the particle sizes shown in the SEM image (Fig.2A). The zeta potential of NIM-loaded MCLN was 16.2 ± 3.1 mV due to the presence of the positively charged component, DOTAP, in the lipid shells. In addition, there was no significant change in the morphology (Fig. S2, Supporting Information), particle size (Table I) and zeta potential (14.7 ± 2.8 mV) of NIM-loaded MCLN after 6 months of storage.

Specific Surface Area and Pore Size Distribution of the Prepared Samples

Nitrogen adsorption/desorption measurements were used to determine the specific surface area, pore size distribution and specific pore volume of the prepared MC and freeze-dried MCLN samples. The nitrogen adsorption/desorption curves and the textural parameters of the materials prepared are shown in Fig. 3 and Table I, respectively. As shown in Fig. 3A, MC particles exhibit a combination of type I and type IV isotherms with a H_1 hysteresis loop at a relatively high pressure, which is characteristic of micro-/mesoporous materials [30, 32]. At lower pressures (P/P_0 below 0.2), the isotherm showed a high degree of adsorption, indicating that the MC nanoparticles possess micropores (type I). However, at higher pressures (P/P_0 = 0.85–0.95), the isotherm exhibited a hysteresis loop, demonstrating the existence of well-defined cylindrical mesopores (type IV) in the frameworks, in accordance with the results obtained from the TEM image (Fig. 1B). Due to the presence of both micropores and mesopores, MC has a high specific surface area and a large pore volume, which were calculated to be 1493 m^2/g and 1.06 cm^3/g by BET and BJH methods, respectively. The large pore volume and surface area indicate that the obtained MC would be excellent if used for hosting more drug molecules [33]. In addition, the successful incorporation of NIM into the pores of the carrier was also confirmed by nitrogen adsorption/desorption measurements. After drug loading, a drastic reduction in specific surface area, pore diameter and pore volume was observed and these changes were attributed to the successful incorporation of NIM into the pores of MC. In addition, the formation of the lipid coating layer was further confirmed by the evidence of pore blocking, in addition to the TEM image shown in Fig.2B. As expected, the surface area and the pore volume of NIM-loaded MCLN samples fell sharply to

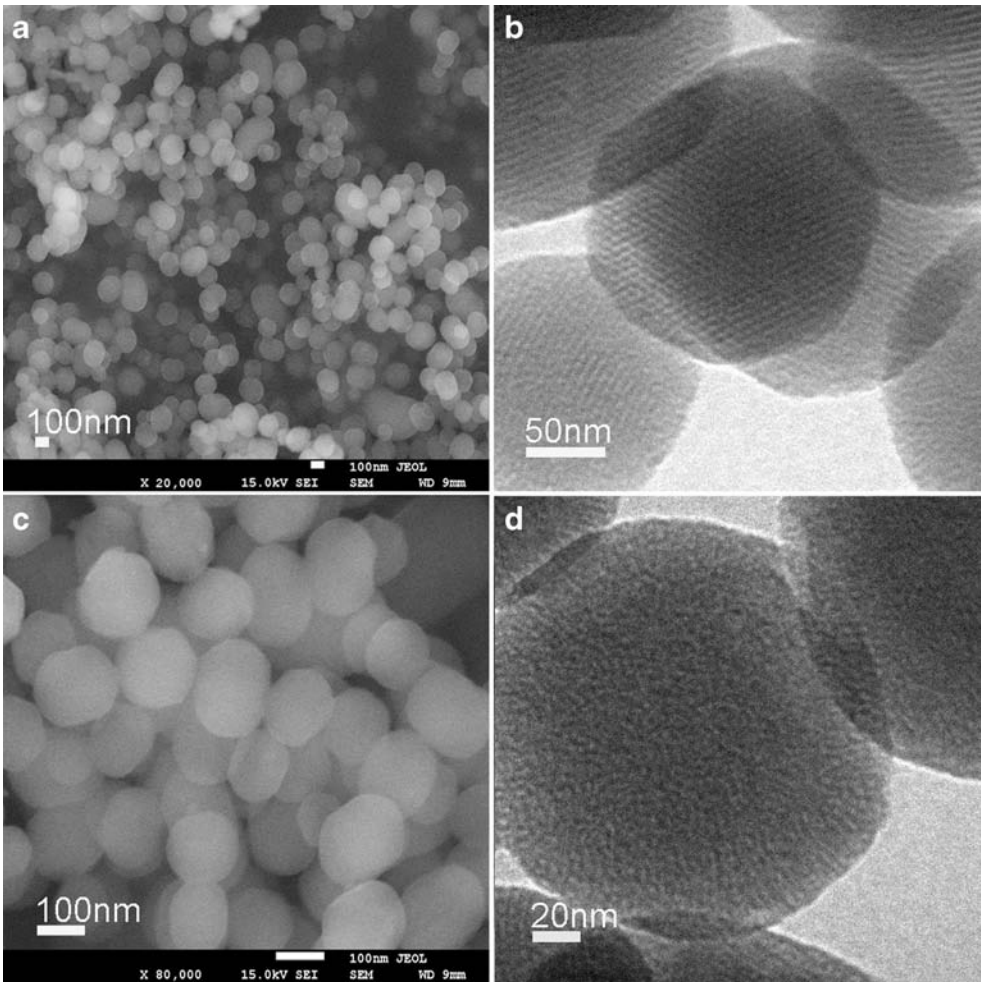

Fig. 1 SEM micrographs of (**A**) MC and (**C**) NIM-MC; TEM micrographs of (**B**) MC and (**D**) NIM-MC.

269 m^2/g and 0.05 cm^3/g, respectively. This result indicates that the entrances to the partial mesoporous channels on the outer surface of NIM-loaded MCLN were indeed enveloped by a liposome shell.

Solid-State Characterization

XRD is an important analytical technique for understanding the amorphous and microcrystalline nature of complex structures. Figure 4 shows comparative diffractograms for coarse NIM, pure MC, the physical mixture of NIM and MC in a 1:2.5 ratio, NIM-loaded MC and freeze-dried NIM-loaded MCLN samples. It can be seen that coarse NIM exhibits characteristic peaks (6.5, 12.8, 17.3, 19.7 and 20.4°) over the 2-theta range in the XRD spectra, whereas pure MC matrices show a broad amorphous band. For the physical mixture, diffraction peaks of NIM were also clearly visible which shows that there was no significant crystal change in NIM (Fig. 4c). However, the diffraction patterns of both NIM-loaded samples showed amorphous halos with an

Table I Specific Surface Area, Pore Diameter, Pore Volume, Particle Size and Drug Loading of the Samples ($n = 3$)

Sample	S_{BET} (m^2/g)	V_t (cm^3/g)	w_{BJH} (nm)	V_{mi} (cm^3/g)	Size (nm)	Drug loading (%)
MC	1493.6 ± 25.1	1.06 ± 0.12	3.0 ± 0.2	0.28 ± 0.04	173 ± 16	–
NIM-MC	427.1 ± 30.5 [a]	0.24 ± 0.07 [a]	1.7 ± 0.4 [a]	0.03 ± 0.01 [a]	178 ± 21	30.1 ± 0.5
NIM-MCLB	269.2 ± 38.1 [a,b]	0.05 ± 0.02 [a,b]	–	–	196 ± 35	27.3 ± 0.6
NIM-MCLB$_1$	230.7 ± 29.5 [a,b]	0.04 ± 0.02 [a,b]	–	–	208 ± 42	27.5 ± 0.5

S_{BET} BET specific surface area, V_t total pore volume, w_{BJH} BJH pore diameter, V_{mi} micropore volume. NIM-MCLB$_1$: NIM-MCLB after 6 months of storage

[a] represent statistically significant differences ($p < 0.05$) compared with MC

[b] represent statistically significant differences ($p < 0.05$) compared with NIM-MC

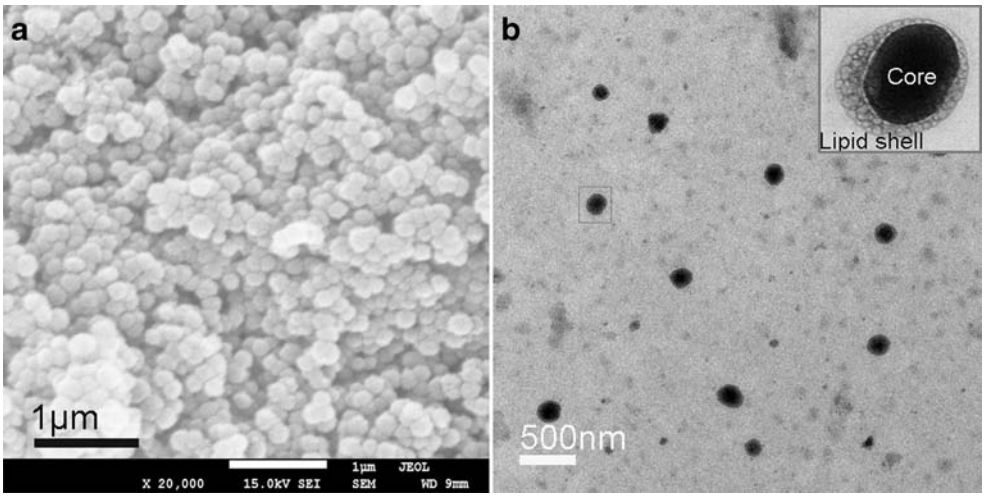

Fig. 2 (**A**) SEM and (**B**) TEM micrographs of NIM-MCLN.

absence of the characteristic crystalline NIM peaks, indicating that the encapsulated drug was in an amorphous state (Fig. 4d and e). This is related to finite-size effects, preventing the drug molecules from rearranging themselves in a crystal lattice [22, 34]. It should be noted that freeze-dried NIM-loaded MCLN showed no sign of recrystallization during the storage period (Fig. 4f). As a result, the stability test showed that freeze-dried NIM-loaded MCLN exhibited good physical stability under accelerated storage conditions for at least 6 months.

The presence or absence of crystalline drug was also confirmed by DSC analysis using the drug melting peak in the thermograms as an indication that NIM in crystalline form was present in the sample. The DSC thermograms of coarse NIM, the physical mixture of NIM and MC in a 1:2.5 ratio, NIM-loaded MC and freeze-dried NIM-loaded MCLN samples are shown in Fig. 5. Coarse NIM displayed one endothermic event, corresponding to the crystal melting from 119 to 131°C. In the DSC heating trace for the physical mixture a similar endothermic peak was also detected (Fig. 5c), suggesting that NIM was present in an unchanged crystalline state in the physical mixture. As expected, no endothermic peak of crystalline NIM was present in the DSC thermograms of both NIM-loaded MC and freeze-dried NIM-loaded MCLN (Fig. 5d and e), indicating that the drug present in the MCLN was in an amorphous state, which agreed well with the XRD results.

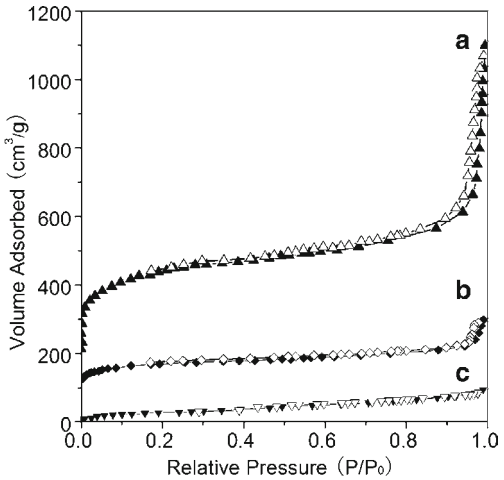

Fig. 3 Nitrogen adsorption/desorption isotherms of (**a**) MC, (**b**) NIM-MC and (**c**) NIM-MCLN. The isotherms of (**a**) and (**b**) were offset vertically by 200 and 100 (cm^3/g), respectively.

Solubility Study

Table II shows the saturation solubility measured for the coarse NIM and NIM-loaded samples. The saturation solubility of coarse NIM was about 2.8±0.3 μg/ml in purified water and 3.6±0.4 μg/ml in PBS (pH 6.8), indicating that NIM is naturally poorly water-soluble. In contrast, both NIM-loaded samples significantly increased the NIM aqueous solubility compared with coarse NIM. NIM-loaded MCLN demonstrated an aqueous solubility of 17.1±1.8 μg/ml in purified water, about 6-fold higher than that of coarse NIM.

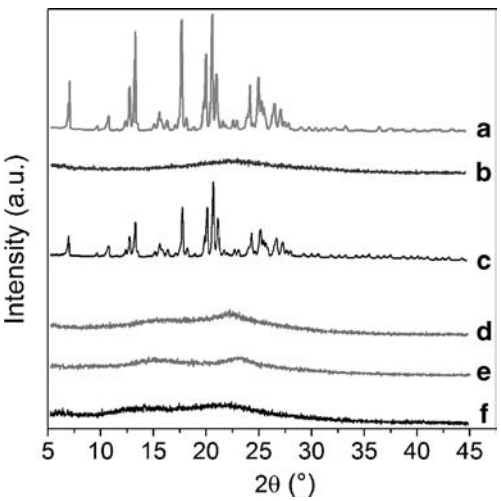

Fig. 4 XRD patterns of (**a**) crude NIM, (**b**) pure MC, (**c**) physical mixture, (**d**) NIM-MC, (**e**) NIM-MCLN and (**f**) NIM-MCLN after 6 months of storage.

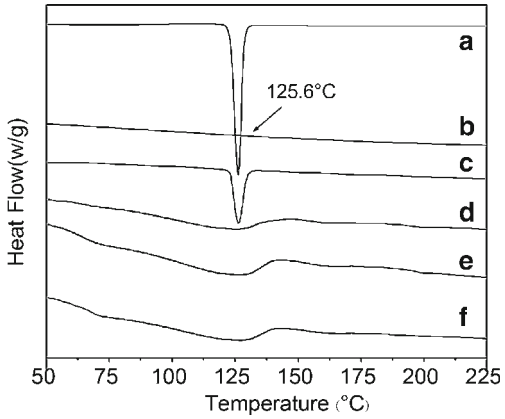

Fig. 5 DSC thermograms of (**a**) crude NIM, (**b**) pure MC, (**c**) physical mixture, (**d**) NIM-MC, (**e**) NIM-MCLN and (**f**) NIM-MCLN after 6 months of storage.

An increase in solubility of the model drug may be largely attributed to changes in the solid state and particle size of NIM. The nano-scale pore channels of the porous matrices converted the crystalline state of NIM to a noncrystalline form (as confirmed by the DSC and XRD results) and reduced the particle size of NIM from the micron range to the low nanometer range (as confirmed by the SEM, TEM and nitrogen adsorption studies), which is known to increase the drug solubility according to the Ostwald–Freundlich equation: log (Cs/C_∞) is proportional to the inverse of r, where Cs is the saturation solubility, C_∞ is the bulk solubility and r is the radius of the drug particles [3, 4, 35]. Moreover, the wetting and solubilization properties of DPPC also helped to dissolve the drug [36]. For the NIM-loaded MCLN sample, no significant change in the aqueous solubility before and after storage was observed.

In Vitro Drug Release Study

The *in vitro* release behavior of NIM from NIM-loaded MCLN in purified water (containing 0.3% SDS), SGF (pH1.2, 0.3% SDS) and SIF (pH6.8, 0.3% SDS) is shown in Fig. 6. The release rate of NIM from NIM-loaded MCLN in different release media was evaluated in comparison with those of the commercial formulation Nimotop®, crystalline NIM and NIM-loaded MC. In purified water, the commercial formulation exhibited a typical immediate-release pattern of NIM under sink conditions. As shown in Fig. 6A, approximately 90% of the drug dissolved from the commercial formulation within just 30 min compared with around 37% for the crystalline NIM samples. In contrast, both NIM-loaded samples displayed a typical sustained release of NIM. For

Table II Saturation Solubilities of Different NIM Formulations (Coarse NIM, NIM-MC and NIM-MCLB) in Aqueous Media ($n = 3$)

Sample	Purified water (μg/ml)	pH 6.8 PBS (μg/ml)
Coarse NIM	2.8 ± 0.3	3.6 ± 0.4
NIM-MC	11.6 ± 1.2 [a]	14.2 ± 1.9 [a]
NIM-MCLB	17.1 ± 1.8 [a]	20.5 ± 2.4 [a]
$NIM\text{-}MCLB_1$	15.9 ± 2.6 [a]	22.5 ± 3.1 [a]

$NIM\text{-}MCLB_1$: NIM-MCLB after 6 months of storage

[a] represent statistically significant differences ($p < 0.05$) compared with coarse NIM

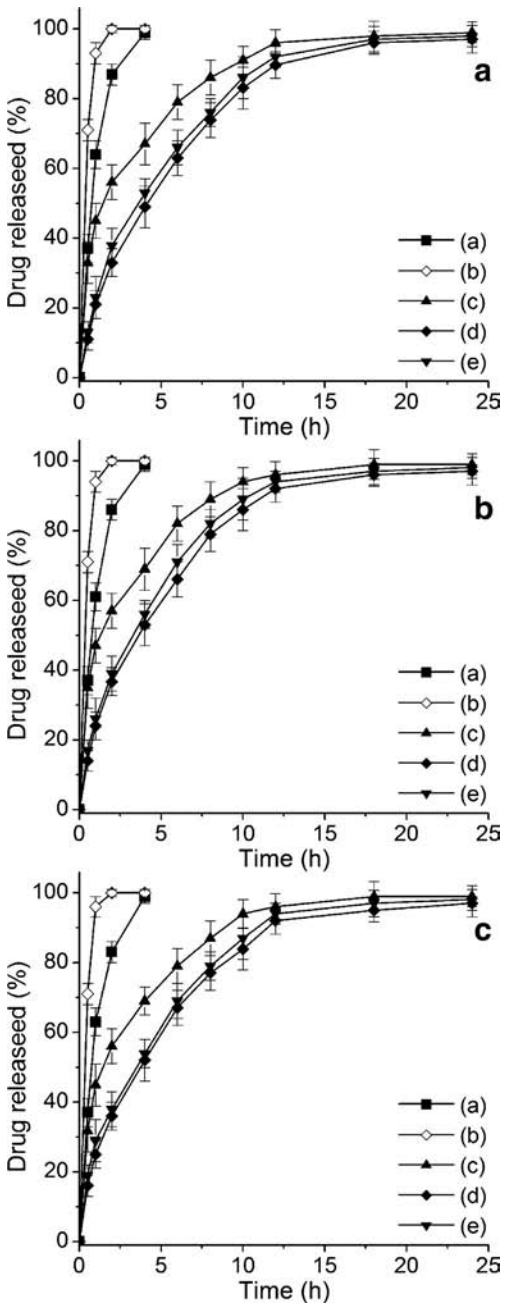

Fig. 6 The release profiles of NIM from different formulations in (**A**) purified water (containing 0.3% SDS), (**B**) SGF (pH1.2, containing 0.3% SDS) and (**C**) SIF (pH6.8,containing 0.3% SDS); (**a**) coarse NIM, (**b**) Nimotop® tablet, (**c**) NIM-MC, (**d**) NIM-MCLN and (**e**) NIM-MCLN (after 6 months of storage). Each data point represents the mean ± SD of three determinations.

the NIM-loaded MC sample, a noticeable biphasic drug release pattern of burst followed by slow release was observed. In the burst release, more than 50% NIM was released within 2 h, which resulted from the fast dissolution of non-encapsulated drug molecules adsorbed on the external surface of MC or hosted at the mesopore openings of MC. In the second stage, the release rate gradually decreased and the cumulative percentage release was close to 100% after 12 h. It is believed that the main reason for the sustained release is due to the micropore and mesopore channels of MC preventing the easy escape of the encapsulated drug molecules from the micro-/mesoporous carbon matrix. As shown in Table I, after drug loading, the micropores of MC almost disappeared. It is well known that drug hosted inside micropores is released very slowly [37]. In addition, due to the small size of the mesopores, the diffusion of solvent into the pores and the counter diffusion of the drug outside the pore channels are severely restricted leading to prolonged drug release [38, 39]. However, it is noteworthy that the release of the freeze-dried NIM-MCLN sample exhibited no dramatic initial burst effect. As seen from the release profile, less than 35% NIM was released during the initial 2 h, then approximately 40% NIM was released over the next 6 h and, finally, almost complete drug release was obtained in about 18 h. This indicated that the coating helped reduce the initial burst release of NIM from the surface of MC by allowing slow penetration of the release medium into the matrix system. As shown in Fig. 6B and C, it is clear that the drug release rate of NIM from NIM-loaded MCLN was not significantly affected by different pH environments. Moreover, the release profiles of NIM from NIM-loaded MCLN were similar to those of freshly prepared ones over a 6 month storage period.

In Vitro Cytotoxicity Assay

In view of the potential utility of MCLN for oral drug delivery applications, the cytotoxicity of MCLN was evaluated using an MTT assay with both Caco-2 and HT-29 cells. As shown in Fig. 7, both MCLN and MC (over a concentration range of 10–200 μg/ml) exhibit no marked cytotoxic effects against Caco-2 or HT-29 cells after incubation for 12 h. When the incubation time was extended to 48 h, MC showed concentration- and time-dependent cytotoxicity effects. In contrast, no significant decrease in cell viability was observed when both types of cell were treated with MCLN under the same conditions. Even at the highest tested concentration (up to 200 μg/ml), MCLN only produced a marginal reduction of about 10% in cell viability. These results suggest that MCLN is more biocompatible than MC due to the presence of the liposome bilayer on the outer surface of MC. Thereafter, MCLN can be safely used for oral drug delivery.

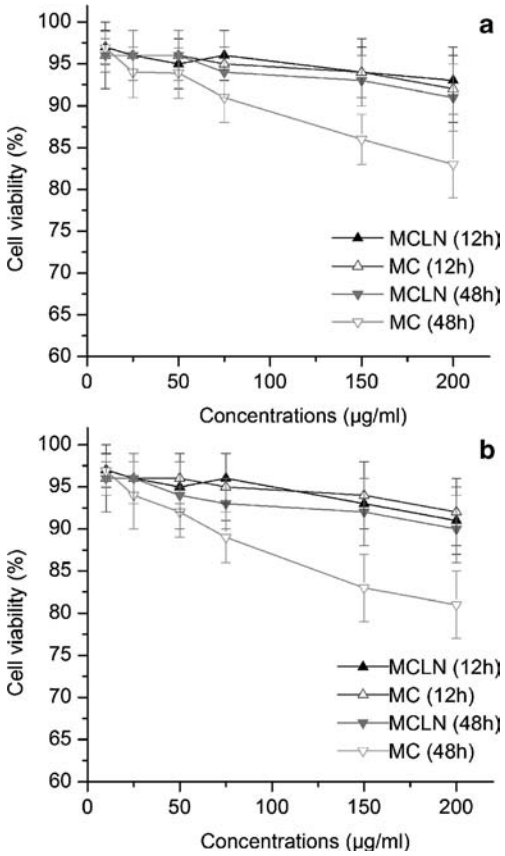

Fig. 7 Cytotoxic effects of MCLN and MC against (**A**) Caco-2 cells or (**B**) HT-29 cells (mean ± SD, $n = 6$).

In-Vivo Absorption Study

The observations on the sustained release and increased saturation solubility properties of NIM-MCLN prompted us to clarify the possible improvement in the absorption of NIM, and, so, the pharmacokinetic profiles of NIM delivered with NIM-MCLN and the immediate release tablets (Nimotop®) were evaluated and compared in dogs under fasting conditions. Figure 8 shows the change in the mean plasma concentration of NIM after oral administration of each NIM formulation, while the mean pharmacokinetic parameters are summarized in Table III. As seen in Fig. 8, there were clear differences in the shape of the concentration *versus* time curves between the NIM-MCLN formulation and the commercial formulation. In the case of the commercial Nimotop® tablets, the plasma level of NIM rose quickly and the maximum concentration was reached after approximately 1 h, followed by a rapid decline and quite low levels were then maintained until 24 h. By comparison, the maximum plasma drug concentration was significantly lower (mean C_{max}, 129.57 ng/ml *versus* 273.61 ng/ml) and was reached later (T_{max}, 4.33 h *versus* 1.42 h) in the case of the NIM-MCLN formulation ($p<0.05$). However, the NIM-MCLN formulation produced higher plasma drug levels from 3 to 24 h compared with the commercial Nimotop® tablets. This result correlated with the sustained drug

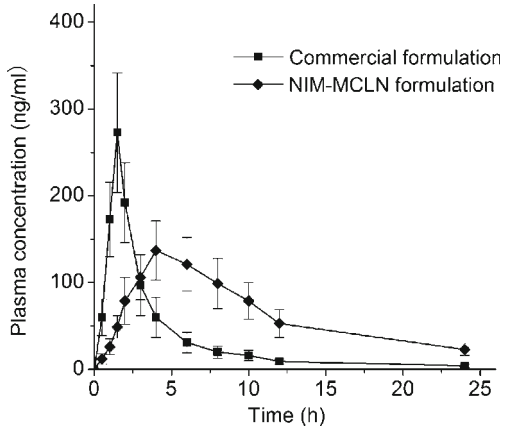

Fig. 8 Plasma concentration–time profiles of NIM in beagle dogs following a single oral administration of different formulations equivalent to 60 mg NIM (mean ± SD, $n = 6$).

release profile of the NIM-MCLN formulation. Both the AUC_{0-24h} and T_{max} values of the NIM-MCLN formulation were markedly higher than those of the commercial formulation, while the C_{max} was lower, indicating that the sustained release NIM-MCLN formulation provides a greater drug exposure and longer sustained plasma drug levels *in vivo*. Interestingly, the relative bioavailability of NIM from the NIM-MCLN formulation was roughly 2.14-fold higher than that from the commercial formulation. The significant increase in oral absorption of NIM for NIM-MCLN was mainly due to its sustained release behavior in the gastrointestinal tract following oral administration and the increased drug solubility induced by the formation of an amorphous state. It is well known that NIM is a substrate for cytochrome P450 isoform3A4 (CYP3A4), while the cytochrome P450 activity progressively decreases along the length of the gut with little to no activity in the colon [40–42]. Therefore, more unmetabolized drug from the NIM-MCLN formulation is available for absorption compared with the commercial formulation. In addition, the high surface area and positive surface charges (16.2 ± 3.1 mV) make the NIM-MCLN nanoparticles more likely to adhere to the gut wall and release drug closer to the epithelium, which can improve oral absorption and lead to increased bioavailability of the encapsulated drug [20, 43, 44].

Table III Pharmacokinetic Parameters of NIM Following a Single Dose of Different NIM Formulations (NIM-MCLN and Nimotop®) (mean ± SD, $n = 6$)

Parameter	NIM-MCLN formulation	Commercial formulation
t_{max} (h)	4.33 ± 0.82*	1.42 ± 0.38
C_{max} (ng/ml)	129.57 ± 33.86*	273.61 ± 69.35
$AUC_{0\rightarrow24h}$ (ng·h/ml)	1597.18 ± 460.50*	752.43 ± 241.62
Relative bioavailability (%)	213.9 ± 50.7	–

Asterisks (*) represent statistically significant differences ($p < 0.05$) compared with the commercial formulation. C_{max} Peak plasma concentration, T_{max} Time taken to reach C_{max}, $AUC_{0\rightarrow24}$ Area under the plasma concentration–time curve from time zero to 24 h

CONCLUSION

In summary, a novel MCLN-based sustained release formulation of NIM was designed, and its morphology, inner structure, specific surface area, pore volume, particle size, drug loading, physical state, aqueous solubility, *in vitro* release behavior, amorphous state stability and pharmacokinetics were studied. Solubility study indicated that NIM-loaded MCLN significantly increased the NIM aqueous solubility compared with crystalline NIM. The NIM-loaded MCLN formulation showed a sustained drug release behavior in simulated intestinal fluid. The *in vivo* absorption study in fasted dogs demonstrated that the NIM-loaded MCLN formulation achieved a greater degree of absorption and longer lasting plasma drug levels compared with the immediate-release formulation. Moreover, MCLN exhibited negligible toxicity in the cytotoxicity assays, confirming the safety of MCLN when used as an oral drug delivery vehicle. This finding could be applied to a far wider range of drugs that exhibit poor aqueous solubility and a short elimination half-life, thus helping improve oral bioavailability and patient compliance through the use of the novel MCLN-based formulation.

ACKNOWLEDGMENTS AND DISCLOSURES

This research was funded by the National Science Foundation of China (No. 81402879), the Natural Science Foundation of Jiangsu Province of China (No. BK20140221), and Project for Excellent Talents in Xuzhou Medical College (No. 53631309). Dr. David B. Jack is gratefully thanked for correcting English of the manuscript. No conflict of interest to be declared by authors.

REFERENCES

1. Lipinski CA, Lombardo F, Dominy BW, Feeney PJ. Experimental and computational approaches to estimate solubility and permeability in drug discovery and development settings. Adv Drug Deliv Rev. 2012;64:4–17.
2. Kawabata Y, Wada K, Nakatani M, Yamada S, Onoue S. Formulation design for poorly water-soluble drugs based on biopharmaceutics classification system: basic approaches and practical applications. Int J Pharm. 2001;420(1):1–10.
3. Nkansah P, Antipas A, Lu Y, Varma M, Rotter C, Rago B, *et al.* Development and evaluation of novel solid nanodispersion system for oral delivery of poorly water-soluble drugs. J Control Release. 2013;169(1–2):150–61.
4. Vasconcelos T, Sarmento B, Costa P. Solid dispersions as strategy to improve oral bioavailability of poor water soluble drugs. Drug Discov Today. 2007;12(23–24):1068–75.

5. Porter CJ, Trevaskis NL, Charman WN. Lipids and lipid-based formulations: optimizing the oral delivery of lipophilic drugs. Nat Rev Drug Discov. 2007;6:231–48.
6. Hill A, Geissler S, Weigandt M, Mader K. Controlled delivery of nanosuspensions from osmotic pumps: zero order and non-zero order kinetics. J Control Release. 2012;158(3):403–12.
7. Chen H, Khemtong C, Yang X, Chang X, Gao J. Nanonization strategies for poorly water-soluble drugs. Drug Discov Today. 2011;16(7–8):354–60.
8. Hamoudi MC, Bourasset F, Domergue-Dupont V, Gueutin C, Nicolas V, Fattal E, *et al.* Formulations based on alpha cyclodextrin and soybean oil: an approach to modulate the oral release of lipophilic drugs. J Control Release. 2012;161(3):861–7.
9. Mehnert W, Mäder K. Solid lipid nanoparticles production, characterization and applications. Adv Drug Deliv Rev. 2001;47(2–3):165–96.
10. Lukyanov AN, Torchilin VP. Micelles from lipid derivatives of water-soluble polymers as delivery systems for poorly soluble drugs. Adv Drug Deliv Rev. 2004;56(9):1273–89.
11. Nguyen TH, Hanley T, Porter CJ, Boyd BJ. Nanostructured liquid crystalline particles provide long duration sustained-release effect for a poorly water soluble drug after oral administration. J Control Release. 2011;153(2):180–6.
12. Zhang Y, Wang J, Bai X, Jiang T, Zhang Q, Wang S. Mesoporous silica nanoparticles for increasing the oral bioavailability and permeation of poorly water soluble drugs. Mol Pharm. 2012;9(3):505–13.
13. Chirra HD, Desai TA. Emerging microtechnologies for the development of oral drug delivery devices. Adv Drug Deliv Rev. 2012;64(14):1569–78.
14. Tan S, Li X, Guo Y, Zhang Z. Lipid-enveloped hybrid nanoparticles for drug delivery. Nanoscale. 2013;5:860–72.
15. Allen TM, Cullis PR. Drug delivery systems: entering the mainstream. Science. 2004;303(5665):1818–22.
16. Su X, Fricke J, Kavanagh DJ, Irvine DJ. In vitro and in vivo mRNA delivery using lipid-enveloped pH-responsive polymer nanoparticles. Mol Pharm. 2011;8(3):774–87.
17. Mendes LP, Gaeti MP, de Ávila PH, de Sousa VM, Dos Santos RB, de Ávila Marcelino RI, *et al.* Multicompartimental nanoparticles for co-encapsulation and multimodal drug delivery to tumor cells and neovasculature. Pharm Res. 2014;31(5):1106–19.
18. Al-Jamal WT, Kostarelos K. Liposomes: from a clinically established drug delivery system to a nanoparticle platform for theranostic nanomedicine. Acc Chem Res. 2011;44(10):1094–104.
19. Wang C, Wang Y, Fan M, Luo F, Qian Z. Characterization, pharmacokinetics and disposition of novel nanoscale preparations of paclitaxel. Int J Pharm. 2011;414(1–2):251–9.
20. Ensign LM, Cone R, Hanes J. Oral drug delivery with polymeric nanoparticles: the gastrointestinal mucus barriers. Adv Drug Deliv Rev. 2012;64(6):557–70.
21. Park J, Fong PM, Lu J, Russell KS, Booth CJ, Saltzman WM, *et al.* PEGylated PLGA nanoparticles for the improved delivery of doxorubicin. Nanomed Nanotech Biol Med. 2009;5(4):410–8.
22. Wani A, Muthuswamy E, Savithra GHL, Mao G, Brock S, Oupický D. Surface functionalization of mesoporous silica nanoparticles controls loading and release behavior of mitoxantrone. Pharm Res. 2012;29(9):2407–18.
23. Zhang Y, Wang H, Li C, Sun B, Wang Y, Wang S, *et al.* A novel three-dimensional large-pore mesoporous carbon matrix as a potential nanovehicle for the fast release of the poorly water-soluble drug, celecoxib. Pharm Res. 2014;31(4):1059–70.
24. Liang C, Li Z, Dai S. Mesoporous carbon materials: synthesis and modification. Angew Chem. 2008;47(20):3696–717.
25. An S, Park JH, Shin CH, Joo J, Ramasamy E, Hwang J, *et al.* Well-dispersed Pd_3Pt_1 alloy nanoparticles in large pore size mesocellular carbon foam for improved methanol-tolerant oxygen reduction reaction. Carbon. 2011;49(4):1108–17.
26. Langley MS, Sorkin EM. Nimodipine. A review of its pharmacodynamic and pharmacokinetic properties, and therapeutic potential in cerebrovascular disease. Drugs. 1989;37:669–99.
27. Chalikwar SS, Belgamwar VS, Talele VR, Surana SJ, Patil MU. Formulation and evaluation of nimodipine-loaded solid lipid nanoparticles delivered via lymphatic transport system. Colloids Surface B. 2012;97(1):109–16.
28. Sun Y, Rui Y, Wenliang Z, Tang X. Nimodipine semi-solid capsules containing solid dispersion for improving dissolution. Int J Pharm. 2008;359(1–2):144–9.
29. Fuhr U, Maier-Bruggemann A, Blume H, Muck W, Unger S, Kuhlmann J, *et al.* Grapefruit juice increases oral nimodipine bioavailability. Int J Clin Pharmacol Ther. 1998;36(3):126–32.
30. Li M, Xue J. Ordered mesoporous carbon nanoparticles with well-controlled morphologies from sphere to rod via a soft-template route. J Colloid Interface Sci. 2012;377(1):169–75.
31. Higuchi T, Connors KA. Phase-solubility techniques. Adv Anal Chem Instrum. 1965;4:117–212.
32. Fang Y, Gu D, Zou Y, Wu Z, Li F, Che R, *et al.* A low-concentration hydrothermal synthesis of biocompatible ordered mesoporous carbon nanospheres with tunable and uniform size. Angew Chem Int Ed. 2010;49(43):7987–91.
33. Yang P, Quan Z, Lu L, Huang S, Lin J. Luminescence functionalization of mesoporous silica with different morphologies and applications as drug delivery systems. Biomaterials. 2008;29(6):692–702.
34. Van Speybroeck M, Mellaerts R, Mols R, Thi TD, Martens JA, Van Humbeeck J, *et al.* Enhanced absorption of the poorly soluble drug fenofibrate by tuning its release rate from ordered mesoporous silica. Eur J Pharm Sci. 2010;41(5):623–30.
35. Dokoumetzidis A, Macheras P. A century of dissolution research: from Noyes and Whitney to the Biopharmaceutics classification system. Int J Pharm. 2006;321(1–2):1–11.
36. May S, Jensen B, Weiler C, Wolkenhauer M, Schneider M, Lehr CM. Dissolution testing of powders for inhalation: influence of particle deposition and modeling of dissolution profiles. Pharm Res. 2014;31(11):3211–24.
37. Hong Y, Chen X, Jing X, Fan H, Guo B, Gu Z, *et al.* Preparation, bioactivity, and drug release of hierarchical nanoporous bioactive glass ultrathin fibers. Adv Mater. 2010;22(6):754–8.
38. Kapoor S, Hegde R, Bhattacharyya AJ. Influence of surface chemistry of mesoporous alumina with wide pore distribution on controlled drug release. J Control Release. 2009;140(1):34–9.
39. Cauda V, Muhlstein L, Onida B, Bein T. Tuning drug uptake and release rates through different morphologies and pore diameters of confined mesoporous silica. Microporous Mesoporous Mater. 2009;118(1–3):435–43.
40. Bailey DG, Malcolm J, Arnold O, Spence JD. Grapefruit juice-drug interactions. Brit J Clin Pharmacol. 1998;46(2):101–10.
41. Peters WH, Kock L, Nagengast FM, Kremers PG. Biotransformation enzymes in human intestine: critical low levels in the colon? Gut. 1991;32(4):408–12.
42. McKinnon RA, McManus ME. Localization of cytochromes P450 in human tissues: implications for chemical toxicity. Pathol (Phila). 1996;28(2):148–55.
43. Davis SS. Formulation strategies for absorption windows. Drug Discov Today. 2005;10(4):249–57.
44. Des Rieux A, Fievez V, Garinot M, Schneider YJ, Préat V. Nanoparticles as potential oral delivery systems of proteins and vaccines: a mechanistic approach. J Control Release. 2006;116(1):1–27.